JBC Papers in Press. Published on November 30, 2017 as Manuscript M117.799536
The latest version is at http://www.jbc.org/cgi/doi/10.1074/jbc.M117.799536

Steady-state analysis of enzymes with non-Michaelis-Menten kinetics. The transport mechanism of Na^+/K^+-ATPase.

José L. E. Monti[1,2], Mónica R. Montes[1,2], Rolando C. Rossi[1,2]

From the [1]Universidad de Buenos Aires, Facultad de Farmacia y Bioquímica, Departamento de Química Biológica and [2]Consejo Nacional de Investigaciones Científicas y Técnicas (CONICET)–Universidad de Buenos Aires, Instituto de Química y Fisicoquímica Biológicas (IQUIFIB). Buenos Aires, Argentina

Running title: *Steady-state analysis of enzymes with non-Michaelis-Menten kinetics*

To whom correspondence should be addressed: JLE Monti, tel.: +54 11 4964 8289 ext. 132, e-mail address: litomonti@gmail.com

Keywords: Non-Michaelis-Menten kinetics, Na^+/K^+-ATPase, allosteric regulation, kinetic mechanisms, steady-state analysis

ABSTRACT

Procedures to define kinetic mechanisms from catalytic activity measurements that obey the Michaelis-Menten equation are well-established. In contrast, analytical tools for enzymes displaying non-Michaelis-Menten kinetics are underdeveloped and transient-state measurements, when feasible, are therefore preferred in kinetic studies. Of note, transient-state determinations evaluate only partial reactions, and these might not participate in the reaction cycle.

Here, we provide a general procedure to characterize kinetic mechanisms from steady-state determinations. We described non-Michaelis-Menten kinetics with equations containing parameters equivalent to k_{cat} and K_M and modeled the underlying mechanism by an approach similar to that used under Michaelis-Menten kinetics.

The procedure enabled us to evaluate whether Na^+/K^+-ATPase uses the same sites to alternatively transport Na^+ and K^+. This *ping-pong* mechanism is supported by transient-state studies but contradicted to date by steady-state analyses claiming that the release of one cationic species as product requires the binding of the other (*ternary-complex* mechanism).

To derive robust conclusions about Na^+/K^+-ATPase transport mechanism, we did not rely on ATPase activity measurements alone. During the catalytic cycle, the transported cations become transitorily occluded (i.e. trapped within the enzyme). We employed radioactive isotopes to quantify occluded cations under steady-state conditions. We replaced K^+ with Rb^+ since $^{42}K^+$ has a short half-life and previous studies showed that K^+- and Rb^+-occluded reaction intermediates are similar. We derived conclusions regarding the rate of Rb^+-deocclusion that were verified by direct measurements.

Our results validated the ping-pong mechanism and proved that Rb^+-deocclusion is accelerated when Na^+ binds to an allosteric, unspecific site, leading to a two-fold increase in ATPase activity.

Regardless of the kinetic mechanism involved, under steady-state conditions, both catalytic activities and concentrations of enzyme reaction intermediates can be expressed as rational functions of the concentration of the reactants (1). For instance, we can express the rate of formation of a product P as a function of the concentration of the varying-reactant A as (2):

$$v_P([A]) = \frac{\sum_{j=0}^{n} \alpha_j [A]^j}{1 + \sum_{j=1}^{d} \beta_j [A]^j} \qquad (1)$$

Michaelis-Menten kinetics is obeyed when the maximum exponent on the concentration of the varying reactant is one, i.e. $\alpha_j = 0$ and $\beta_j = 0$ for every $j > 1$. This holds for reaction schemes where the

varying reactant binds to only one enzyme reaction intermediate. Non-Michaelis-Menten kinetics occurs, for instance, when the varying reactant is both substrate and inhibitor (substrate inhibition) or participates in alternative productive pathways or, with some exceptions, when its stoichiometric coefficient is higher than one.

Most reported enzymes seem to follow Michaelis-Menten kinetics. An enlightening literature search of kinetic studies performed in the period 1965-1976 (3), found non-Michaelis-Menten kinetics in approximately 800 enzymes, i.e. 20% of the total known at that time. Nevertheless, we think it remains valid today what was pointed out by the authors regarding that Michaelis-Menten kinetics is usually not verified and that the proportion of enzymes with non-Michaelis-Menten kinetics is therefore probably much higher.

The analysis of kinetic mechanisms in enzymes with Michaelis-Menten kinetics is widely described (4, 5). Briefly, the Michaelis-Menten equation is fitted to data of catalytic activity measured varying the concentration of one substrate (variable substrate) at different fixed concentrations of one of the others (changing fixed substrate), while keeping all other substrates, if there are any, at constant concentration. Then, fitted values of parameters k_{cat}/K_M and K_M are plotted against the concentration of the changing fixed substrate. The patterns obtained give insights into the kinetic mechanism involved. For instance, for a bi-substrate enzyme, it is possible to realize whether both substrates must bind to the enzyme before giving any products (ternary-complex mechanism) or not (ping-pong mechanism). When products are absent, if K_M tends to zero as the concentration of the changing fixed substrate tends to zero then the mechanism is ping pong. Otherwise, it is a ternary-complex mechanism.

Reaction schemes for enzymes with non-Michaelis-Menten kinetics are generally assembled from transient-state results since there is no validated procedure to do this from steady-state determinations. Transient-state studies provide very valuable information but are more difficult to perform and they evaluate only partial reactions, which might not be part of the reaction cycle. Here we provide a general procedure to characterize enzymes with non-Michaelis-Menten kinetics by an approach similar to that used under Michaelis-Menten kinetics. The procedure enabled us to evaluate whether Na^+/K^+-ATPase uses the same sites to alternatively transport Na^+ and K^+.

Na^+/K^+-ATPase is a transmembrane enzyme (6–9) that under physiological conditions couples the hydrolysis of one intracellular ATP molecule (into ADP and orthophosphate) to the exchange of three intracellular Na^+ (Na_i^+) for two extracellular K^+ (K_e^+). During the catalytic cycle the enzyme undergoes phosphorylation and dephosphorylation and the transported cations become transitorily occluded (trapped within the enzyme). The currently accepted Albers-Post model (Figure 1) poses that the binding of 3 Na_i^+ to the intermediate E1ATP triggers its phosphorylation leading to E1P(Na_3^+), which spontaneously undergoes a conformational change to give E2P, thereby releasing Na^+ cations to the extracellular side. The binding of 2 K_e^+ to E2P leads to its dephosphorylation and the concomitant occlusion of the cations. The K^+-occluded intermediates are very stable, making the release of K^+ towards the intracellular side the rate limiting step of the reaction cycle.

The Albers-Post model poses that Na^+ and K^+ are alternatively transported by the same set of sites (10–12). This ping-pong nature of the transport is supported by few studies on partial reactions of the catalytic cycle (13–16). However, many other studies evaluating the global functioning of the pump by steady-state measurements supported ternary-complex mechanisms (17–29), with at least one reaction intermediate with Na_i^+ and K_e^+ simultaneously bound to their transport sites. As far as we know, the ping-pong mechanism has not been corroborated to date by steady-state measurements.

ATPase activity measurements at varying concentrations of the transported cations would give enough information to address the question of the transport mechanism. However, we perceived that the complexity of the kinetic mechanism of Na^+/K^+-ATPase demanded complementary assays to derive robust conclusions and explain some unexpected results. Therefore, we included steady-state and transient-state determinations of the amount of the K^+ congener Rb^+ (15) that is trapped within enzyme reaction intermediates. Briefly, we proceeded as follows. We fitted rational functions of the concen-

tration of Na^+ (variable substrate) to measurements of both ATPase activity and steady-state amounts of occluded Rb^+, at different fixed concentrations of Rb^+ (changing fixed substrate). Fitted values of parameters equivalent to k_{cat}/K_M and K_M were then plotted versus the concentration of Rb^+ to conclude, from the pattern obtained, whether the transport responds to a ping-pong or a ternary-complex mechanism. We did this analysis either in the absence or in the presence of 2 mM ADP. Results in the absence of ADP served as a control since under this condition the system must give the ping-pong pattern, regardless of the transport mechanism involved (see *Theory* below). Moreover, fitted values of other parameters allowed us to predict values for the velocity constants of Rb^+ deocclusion. The predicted values agreed with those obtained by direct measurements, giving consistency to the whole analysis.

Our results validated the ping-pong nature of the transport mechanism from steady-state determinations. Additionally, we found that Rb^+ deocclusion is accelerated when Na^+ binds to an allosteric, unspecific site, leading to a two-fold increase in ATPase activity. It is very likely that the effects of the binding of Na^+ to this allosteric site have been wrongly attributed to the occupancy of its transport sites, which led to propose a ternary-complex transport mechanism.

RESULTS AND DISCUSSION

Theory — Here, we will illustrate how ping-pong and ternary-complex mechanisms are differentiated under Michaelis-Menten- and non-Michaelis-Menten kinetics.

Figure 2 shows representative models for the transport of Na^+ and the K^+ congener Rb^+ by Na^+/K^+-ATPase. Figure 2A shows a ping-pong model based on that of Albers and Post, whereas Figures 2B and 2C show two ternary-complex models that are compatible with the empirical evidence that originally led to the Albers-Post model, i.e.: i) Na^+ is required for enzyme ATP-dependent phosphorylation and ii) K^+ is required for enzyme dephosphorylation (26).

When the stoichiometry for transport is set to 1 Na^+_i for 1 Rb^+_e and the concentration of the products Na^+_e and Rb^+_i is set to zero, all models follow Michaelis-Menten kinetics and, for a fixed concentration of Rb^+_e, the velocity of formation of the product Pi per unit of total enzyme concentration (molar catalytic activity) can be expressed as

$$Act([Na^+_i]) = \frac{1}{[E_{total}]}\frac{d[Pi]}{dt} = \frac{k_{catNai}\dfrac{[Na^+_i]}{K_{MNai}}}{1+\dfrac{[Na^+_i]}{K_{MNai}}} \quad (2)$$

where k_{catNai} is the catalytic constant and K_{MNai} is the Michaelis-Menten constant.

As summarized in Table 1, the dependence of the ratio k_{catNai}/K_{MNai} and K_{MNai} with the concentration of the fixed substrate Rb^+_e varies with the model considered (30). For the ping-pong model, as $[Rb^+_e]$ approaches zero the ratio k_{catNai}/K_{MNai} tends to a positive value while K_{MNai} becomes zero. Unless both ADP and Pi are absent (this is discussed below), ternary-complex models exhibit a different pattern: when $[Rb^+_e]$ approaches zero, the ratio k_{catNai}/K_{MNai} tends to zero whereas K_{MNai} does not. This kind of analysis was originally proposed by Cleland (4, 5) and they are part of what is known as Cleland's rules.

When the concentration of the products Na^+_e and Rb^+_i is zero but the stoichiometry for transport is 3 Na^+_i for 2 Rb^+_e as posed in Figure 2, we obtain a rational equation of higher complexity:

$$Act([Na^+_i]) = \frac{a_{Nai3}\dfrac{[Na^+_i]^3}{K_{Nai1}K_{Nai2}K_{Nai3}}}{1+\dfrac{[Na^+_i]}{K_{Nai1}}+\dfrac{[Na^+_i]^2}{K_{Nai1}K_{Nai2}}+\dfrac{[Na^+_i]^3}{K_{Nai1}K_{Nai2}K_{Nai3}}} \quad (3)$$

Here, the parameters K_{Nai1}, K_{Nai2}, and K_{Nai3} are the apparent stepwise dissociation constants of the enzyme for Na^+_i and, like K_{MNai}, they have concentration units. The meaning of a_{Nai3} is equivalent to that of k_{catNai} in Equation 2, although this is not always true, for instance, in branched models (see Supplementary Material). As in the case of k_{catNai}, the units of a_{Nai3} are those of the catalytic activity, *Act*.

In Equation 3, the dependence of $a_{Nai3}/(K_{Nai1}K_{Nai2}K_{Nai3})$ and $K_{Nai1}K_{Nai2}K_{Nai3}$ with $[Rb^+_e]$ is respectively the same as that of k_{catNai}/K_{MNai}

and K_{MNai} in Michaelis-Menten models (cf. Eqs. S1-S2, S5-S6, and S9-S10, to Eqs. S13-S14, S18-S19, S23-S24, in Supplementary Material).

The ping-pong pattern (see Table 1) results from the fact that the denominator in the steady-state equations lacks a term independent of the concentrations of both substrates, Na_i^+ and Rb_e^+. This occurs whenever the reaction scheme contains irreversible steps interposed between those in which the substrates bind (4). Consequently, in the absence of both ADP and Pi, all three models in Figure 2 will display the ping-pong pattern (31). When both ADP and Pi are present and both products Na_e^+ and Rb_i^+ are absent, the only scheme in Figure 2 showing the ping-pong pattern will be the ping-pong model in panel A. Therefore, to truly distinguish between ping-pong and ternary-complex mechanisms, ADP and/or Pi must be present in the reaction.

When working with non-compartmentalized preparations, the concentrations of a transported substance as substrate and product are necessarily equal and cannot be manipulated independently. In our system $[Na_i^+] = [Na_e^+] = [Na^+]$ and $[Rb_e^+] = [Rb_i^+] = [Rb^+]$. The presence of products Na_e^+ and Rb_i^+ is thus unavoidable and will reverse the reaction steps that involve their release. Furthermore, Na^+ and Rb^+ compete for both intracellular and extracellular transport sites of the enzyme. Under the conditions described, equations for models in Figure 2 change. In fact, even if stoichiometry for transport is set to 1 Na_i^+ for 1 Rb_e^+, models no longer follow Michaelis-Menten kinetics. In the absence of ADP or Pi, they give

$$Act([Na^+]) = \frac{a_{Na1}\dfrac{[Na^+]}{K_{Na1}}}{1 + \sum_{j=1}^{d} \dfrac{[Na^+]^j}{\prod_{g=1}^{j} K_{Nag}}} \qquad (4)$$

where $d = 2$ and 3 in ping-pong and ternary-complex models, respectively.

If stoichiometry for transport is 3 Na_i^+ for 2 Rb_e^+, we obtain:

$$Act([Na^+]) = \frac{a_{Na3}\dfrac{[Na^+]^3}{K_{Na1}\,K_{Na2}\,K_{Na3}}}{1 + \sum_{j=1}^{d} \dfrac{[Na^+]^j}{\prod_{g=1}^{j} K_{Nag}}} \qquad (5)$$

where $d = 6$ and 8 in ping-pong and ternary-complex models, respectively.

Despite the differences in the form of the equations for non-compartmentalized systems (cf. Equations 2-3 and 4-5), for $[Rb^+]$ tending to zero the critical features in the patterns remain unchanged. In the ping-pong pattern, the ratios a_{Na1}/K_{Na1} and $a_{Na3}/(K_{Na1}K_{Na2}K_{Na3})$ tend to non-zero values whereas K_{Na1} and $K_{Na1}K_{Na2}K_{Na3}$ tend to zero. Conversely, in the ternary-complex pattern the ratios a_{Na1}/K_{Na1} and $a_{Na3}/(K_{Na1}K_{Na2}K_{Na3})$ tend to zero while K_{Na1} and $K_{Na1}K_{Na2}K_{Na3}$ tend to non-zero values (see Table 1; proof for this is given under Supplementary Material, Eqs. S3-S4, S7-S8, S11-S12, S15-S16, S20-S21, and S25-S26). Therefore, ping-pong and ternary-complex mechanisms are still distinguishable, remarkably, despite the reversibility of the steps that involve the release of Na^+ and Rb^+ as products.

Another important aspect to consider is that Na^+/K^+-ATPase also hydrolyses ATP by reaction pathways other than the physiological one (10, 11, 32, 33): i) X/X-ATPasic cycling mode, in the absence of alkaline cations (34, 35); ii) X/Rb^+-ATPasic cycling mode, when Rb_e^+ is transported in the absence of Na^+ (33, 36, 37); iii) Na^+/Na^+-ATPasic cycling mode, when the enzyme exchanges Na_i^+ for Na_e^+ (22, 33, 38, 39); iv) other reactions pathways where Na_i^+ triggers enzyme phosphorylation but is followed by spontaneous dephosphorylation (uncoupled sodium efflux) (35, 40–43) or by dephosphorylation stimulated by a single Rb^+ (44). Equations from models containing alternative cycling modes show that some of these affect the parameters to the point that they can make both $a_{Na3}/(K_{Na1}K_{Na2}K_{Na3})$ and $K_{Na1}K_{Na2}K_{Na3}$ to tend to non-zero values as $[Rb^+]$ tends to zero (cf. Eqs. S15 with S27 and S21 with S32 in Supplementary Material) thus undermining the possibility to discriminate ping-pong from ternary-complex mechanisms using the criteria in Table 1. We will show that the influence of alternative cycling modes can be neglected in our system.

The roles of ADP — As mentioned before, to truly distinguish between ping-pong and ternary-complex mechanisms, the products ADP and/or Pi must be present in the reaction to avoid irreversible steps between the binding of Na^+ and Rb^+ as sub-

strates. It can be shown that to make the distinction between the ping-pong model in Figure 2A and the ternary-complex model in Figure 2B it is required the presence of ADP (see Eq. S21 in Supplementary Material), whereas if the ternary-complex model is that in Figure 2C, it is required the presence of Pi (see Eq. S25 in Supplementary Material). Nevertheless, the model shown in Figure 2C assumes that binding of Na_i^+ is essential for the release of Rb^+, which contrasts with the evidence shown both in the literature (15) and later in this work (see Figure 5). For this reason, we will only consider the ternary-complex model in Figure 2B as an alternative to the ping-pong model.

Since ADP is needed to distinguish between these mechanisms, we must take into consideration that this nucleotide plays a dual role: not only as product of the ATP-dependent phosphorylation step but also as a competitor of ATP for the nucleotide binding sites in E1 and E2(Rb_2^+) (15, 31, 45).

In Figure 3A we show the dependence of Na^+-ATPase activity with [ATP] when measured in the presence of 2 mM ADP. When [ATP] is higher than around 1 mM, Na^+-ATPase activity almost reaches its maximum, meaning that most of the ADP has been displaced by ATP from the nucleotide binding sites in E1. The effect of 2 mM ADP on ATPase activity measured at 2.5 mM ATP is therefore mainly due to the reversion of the phosphorylation step.

Both ATP and ADP bind to Rb-occluded intermediates leading to an increase in the rate of Rb^+ deocclusion, but ADP is not as effective as ATP and binds with lower affinity (15). Figure 3B shows that at 2.5 mM ATP, the apparent velocity constant of Rb^+ deocclusion, $k_{app\text{-}deocc}$, decreases slightly with the concentration of ADP.

Based on these results, ADP effects on the reaction cycle other than the reversion of the phosphorylation step are minimized when using ATP and ADP concentrations of 2.5 and 2 mM, respectively.

ATPase activity and levels of occluded Rb^+. General properties of the catalytic mechanism — We performed parallel measurements of ATPase activity (*Act*) and steady-state levels of occluded Rb^+ (*Occ*) as a function of [Na^+] at different fixed [Rb^+]. Reaction media contained 2.5 mM ATP, 0 or 2 mM ADP, and CholineCl to keep constant the ionic strength. For each [Rb^+], *Act* and *Occ* were adequately described by rational equations (see Equations 7 and 8) with the same denominator, as expected if both measurements expressed steady-state properties of the same enzyme (see for instance references (1) and (46) and Supplementary Material).

Here, we will make a qualitative analysis of representative *Act* and *Occ* curves at Rb^+ concentrations arbitrarily classified as *low* (approximately between 0.03 and 0.3 mM) and *high* (approximately above 1 mM). We will focus on the predominant cycling modes of the enzyme under the experimental conditions tested.

Figure 4A shows the results of a typical experiment performed at *low* [Rb^+]. In the absence of Na^+, both *Act* and *Occ* have small but significant non-zero values as a result of the X/Rb^+-ATPasic cycling mode (33–37), where the enzyme couples the hydrolysis of ATP to the occlusion and transport of Rb^+. As [Na^+] increases, *Act* and *Occ* curves exhibit a correlated increase due to the transition towards the physiological Na^+/Rb^+-ATPasic cycling mode. Further increments in [Na^+] causes a correlated decrease in these curves which are easily explained by posing that Na^+ displaces Rb^+ from its transport sites in E2P reducing both the level of occluded-Rb^+ and the rate of enzyme dephosphorylation. When [Na^+] is increased even more, the Na^+/Na^+-ATPasic cycling mode (exchanging 3 Na_i^+ for 2 Na_e^+) starts to prevail (22, 33, 39), resulting in an increase in *Act*, while *Occ* tends to zero.

Figure 4B shows the results of a typical experiment performed at *high* [Rb^+]. At null [Na^+], there is a substantial occlusion of Rb^+ through the direct route, i.e. without formation of phosphoenzyme. The strong accumulation of intermediates occluding Rb^+ inhibits the ATPase activity given by the X/Rb^+-ATPasic cycling mode (33, 36, 37). When [Na^+] is raised, *Act* and *Occ* curves exhibit a correlated increase due to the transition towards the physiological Na^+/Rb^+-ATPasic cycling mode. Further increments in [Na^+] lead to a decrease in *Occ* that is less steep than that observed at *low* [Rb^+] and is correlated not to a decrease but to a considerable increase in ATPase activity. These effects of Na^+ cannot be attributed to a transition towards the Na^+/Na^+-ATPasic cycling mode (expected to take place at much higher [Na^+]) but to the fact that Na^+

binds with low affinity to the Rb-occluded intermediate and promotes Rb^+ deocclusion, which is the rate limiting step of the Na^+/Rb^+-ATPasic cycling mode (see Figure 5 and references (15, 47, 48)).

The continuous lines that describe the results of ATPase activity in Figure 4 respond to equations of the form of Equation 7 with $n = d$ (see *Experimental procedures*). When the denominator (*denom*) is distributed among the numerator terms, *Act* can be expressed as

$$Act([Na^+]) = \sum_{j=0}^{n} v_{Naj} \qquad (6)$$

with n equal to 5 or 4 for *low* and *high* $[Rb^+]$, respectively, and

$$v_{Naj} = \frac{a_{Naj}\dfrac{[Na^+]^j}{\prod_{g=1}^{j} K_{Nag}}}{denom}$$

v_{Naj} terms estimate the flux of the reaction through specific cycling modes and are plotted in Figure 4C and 4D. At *low* $[Rb^+]$, ATPase activity is mostly given by v_{Na3} and, at *high* $[Rb^+]$, by the sum of v_{Na3} and v_{Na4}. As we show in *Comparison of global and partial reactions* below, the terms v_{Na3} and v_{Na4} mainly reflect the contribution to *Act* of the Na^+/Rb^+-ATPasic cycling mode that takes place, respectively, without or with the low affinity binding of Na^+ to the Rb-occluded intermediate. The sum $v_{Na0} + v_{Na1} + v_{Na2} = v_{Na012}$ is given by cycling modes where the enzyme is phosphorylated through pathways other than the physiological one, whereas v_{Na5} is mostly given by the Na^+/Na^+-ATPasic cycling mode, i.e. exchange of 3 Na^+_i for 2 Na^+_e.

Comparison of global and partial reactions — To evaluate if the binding of Na^+ to the Rb-occluded intermediate can account for the low affinity increase in ATPase activity observed in Figure 4B (v_{Na4} in Figure 4D), we measured the time course of Rb^+ deocclusion at different concentrations of Na^+ and obtained the apparent velocity constant of the process ($k_{app\text{-}deocc}$). Figure 5 shows (empty circles) that $k_{app\text{-}deocc}$ increases from 10 s^{-1} in the absence of Na^+ to about 24 s^{-1} at 100 mM Na^+ and then decreases very slightly with further increments in the cation concentration. We have included the results of a similar experiment performed in the presence of 5 mM RbCl (filled circles). Our results suggest that Na^+ and Rb^+ compete for the same site(s) since their effects on $k_{app\text{-}deocc}$ are not additive (the effect of Rb^+ tends to disappear as $[Na^+]$ increases). As previously reported (15), not only Na^+ but also other alkali cations, including Rb^+, increase $k_{app\text{-}deocc}$ to a similar extent supporting the allosteric nature of the binding site.

We have solved models like those in Figure 2A and 2B but including both alternative cycling modes (e.g., X/X-, X/Rb^+- or Na^+/Na^+-ATPasic cycling modes) and the binding of Na^+ to E2(Rb^+_2)ATP as a putative activator of Rb^+ deocclusion, like in the scheme in Figure 5B. The models lead to more complex equations with the form of Equations 7 and 8. The solutions are given under Supplementary Material (see models PP1 and TC2). When alternative cycling modes are canceled, both models predict that in the absence of ADP (see Eqs. S29-S30 and S34-S35, in Supplementary Material):

$$a_{Na3}/(o_{Na3}/2)_{[ADP]=0} = k_{deocc}$$

and

$$a_{Na4}/(o_{Na4}/2)_{[ADP]=0} = k_{deoccna}$$

As these equalities are met only when cycling modes other than the physiological one are neglected, they are a good test for the contribution of such modes to the terms v_{Na3} and v_{Na4} above.

Values for $a_{Na3}/(o_{Na3}/2)$ and $a_{Na4}/(o_{Na4}/2)$ were obtained from the fitting of Equations 7 and 8 to the whole set of results of *Act* and *Occ* as described under *Empirical equations*. Figure 6 shows that fitted curves reproduced very well the results (parameter values are given in Table 3). From results obtained in the absence of ADP, $a_{Na3}/(o_{Na3}/2)$ was 10.1 ± 0.2 s^{-1} regardless of $[Rb^+]$, whereas $a_{Na4}/(o_{Na4}/2)$ was 22.1 ± 0.6 s^{-1} at 5 mM Rb^+. These values are in very good agreement with those of k_{deocc} (10.4 ± 0.9 s^{-1}) and $k_{deoccna}$ (23.4 ± 0.8 s^{-1}) respectively, given by model in Figure 5B when fitted to direct measurements of $k_{app\text{-}deocc}$ (see continuous line in Figure 5A; model parameters values are listed in Table 2).

The analysis above confirms, at least for measurements performed at zero [ADP], that the contribution of alternative cycling modes to v_{Na3} is

negligible for all [Rb^+] tested whereas this is true for v_{Na4} only at *high* [Rb^+].

Noteworthy, the agreement between the values of $a_{Na3}/(o_{Na3}/2)_{[ADP]=0}$ and $k_{app\text{-}deocc}$ at zero [Na^+] (k_{deocc} in Figure 5B) indicates that the binding of Na^+ to the Rb-occluded intermediate is not essential for the release of Rb^+_i during the ATP-driven exchange of 3 Na^+_i for 2 Rb^+_e. In other words, Na^+-independent deocclusion of Rb^+ is compatible with the turnover rate of the enzyme. Moreover, the simple assumption of the existence of an allosteric site for Na^+ in E2(Rb^+_2)ATP explains qualitatively and quantitatively both the activation of Rb^+ deocclusion and the significant contribution of v_{Na4} at *high* [Rb^+].

Validation of the ping-pong mechanism for the transport of Na^+ and K^+ by steady-state determinations — To validate the ping-pong mechanism, we evaluated the pattern obtained for parameters $a_{Na3}/(K_{Na1}K_{Na2}K_{Na3})$ and $K_{Na1}K_{Na2}K_{Na3}$ as a function of [Rb^+]. In one set of experiments, we omitted both ADP and Pi as a control of the ping-pong pattern. In another set, media contained enough ADP as to reverse the phosphorylation step, bringing to a minimum its effects as a competitor of ATP for the nucleotide binding sites in E1 and E2(Rb^+_2) (see Figure 3). Figure 6 shows the fitting of empirical equations to the complete set of results for ATPase activity and occluded Rb^+ as a function of [Na^+] at different Rb^+ concentrations, as described under *Experimental procedures*. Addition of 2 mM ADP to the reaction medium causes ATPase activity to decrease by nearly one-half, evidencing the reversion of the ATP-driven phosphorylation step.

Figure 7 shows the dependence of the fitted values of the parameters $a_{Na3}/(K_{Na1}K_{Na2}K_{Na3})$ and $K_{Na1}K_{Na2}K_{Na3}$ on [Rb^+] in the absence and in the presence of ADP. The results clearly validate the ping-pong nature of the transport mechanism of Na^+/K^+-ATPase. Notably, the product $K_{Na1}K_{Na2}K_{Na3}$ tends to zero as [Rb^+] tends to zero (Table 1).

A model to describe the results — Figure 8 shows a ping-pong model for the active transport of three Na^+ for two Rb^+ cations. The model includes alternative cycling modes that were extensively studied elsewhere in our system (33). The continuous lines in Figure 9 are the plot of model equations fitted to the results shown in Figure 6. The values for the parameters are listed in Table S1 under Supplementary material.

The physiological cycling mode is given by the reaction cycle E1ATP → E1P(Na^+_3) → E2P → E2(Rb^+_2)ATP → E1ATP. The ping-pong nature of the model becomes evident by noting that binding of Na^+_i (Rb^+_e) to transport sites is not mandatory for Rb^+ (Na^+) to be released from the enzyme as product. We included in the model the allosteric binding of one Na^+ ion to the Rb-occluded state, E2(Rb^+_2)ATP. This binding increases the velocity of Rb^+ release since $k_{deoccna} > k_{deocc}$ (see Table S1 in Supplementary Material) and is responsible for an important fraction of the ATPase activity given by the physiological cycling mode at [Na^+] higher than 50 mM.

Dotted lines in Figure 9 show the contribution of the physiological cycle to ATPase activity, and is calculated as $k_{4rb2}\, fp_{rb2}$ [E2P] (see Figure 8). As [Rb^+] tends to infinity, this contribution approaches ATPase activity, i.e. alternative cycling modes tend to vanish.

FINAL REMARKS

We characterized the kinetic mechanism of Na^+/K^+-ATPase from steady-state determinations. The analytical procedure we implemented here is also valid for other membrane transport ATPases. Of note, we used a non-compartmentalized enzyme preparation since the transported substances as products do not interfere with the analysis.

To describe non-Michaelis-Menten kinetics, we found very useful to reparametrize the equation recommended by the International Union of Biochemistry (IUB, now IUBMB), which has not been revised since 1981 (49). We proposed parameters that facilitate predicting the trace of the curve from their values and vice versa. For example, parameter a_{Nai3} in Equation 3 equals the limiting value of *Act* when [Na^+_i] tends to infinity. An approximate value of parameter a_{Nai3} is therefore easy to guess from visual inspection of the results. This facilitates the selection of the equation that best reproduces the results. In contrast, the equation recommended by the IUBMB (Equation 1) contains the parameter α_3 which equals $a_{Nai3}/(K_{Nai1}K_{Nai2}K_{Nai3})$ and, as a consequence, is difficult to guess an approximate value

for it.

In addition, we identified parameters that report key features the reaction scheme must have to reproduce the results. The parameters exhibit the same patterns as those of k_{cat}/K_M and K_M in the classical Michaelis-Menten equation. Therefore, it is possible to use the same general approach to analyze both Michaelis-Menten and non-Michaelis-Menten kinetics. Of note, the analytical procedure we described here is a "model free" strategy (it does not require to pose models *a priori*) and is valid for the kinetic analysis of any other system.

The complexity of the kinetic mechanism of Na^+/K^+-ATPase prevented previous attempts to solve it by steady-state approaches. In this sense, Sachs (14) pointed out that the existence of an uncoupled Na^+ efflux makes impossible the use of standard steady-state methods to confirm the ping-pong nature of the mechanism. Although this statement is mathematically correct (see models PP1 and TC2 under Supplementary Material), we have shown here that the impact of alternative cycling modes on those parameters that are crucial for assigning a kinetic mechanism is negligible. This is evidenced by the fact that one of the parameters of analysis, $K_{Na1}K_{Na2}K_{Na3}$, approaches zero when $[Rb^+]$ tends to zero (as discussed under *Theory*). We gave further support for disregarding the impact of alternative cycling modes by proving that $a_{Na3}/(o_{Na3}/2)$ at zero [ADP] equals the Na^+-independent rate of Rb^+ deocclusion.

We obtained values for $a_{Na3}/(o_{Na3}/2)$ from parallel determinations of ATPase activity and steady-state levels of occluded Rb^+. This is the first study that performed determinations of Rb^+-occluded intermediates at varying concentrations of the transported cations during the hydrolysis of ATP.

We proved the ping-pong nature of the transport mechanism from steady-state determinations. To date, the ping-pong mechanism was supported by few transient-state studies (13–16) and suggested by crystal structures of the enzyme occluding two Rb^+ (6, 7) or three Na^+ (8, 9) cations. Crystallographic analysis indicated that transport sites for Na^+ and Rb^+ share some of the binding residues (8), suggesting that it is not possible to form a ternary-complex.

Although the release of Rb^+ does not require Na^+ to complete the Na^+/Rb^+-ATPase cycle, we found that the allosteric effect of Na^+ on the deocclusion rate accounts for an increase of almost twice in ATPase activity. This significant effect might explain why many authors misinterpreted this kind of results as proof of a ternary-complex mechanism.

The presence of an allosteric site has also been suggested in previous kinetic and structural works. Forbush showed (15) that the allosteric effect on $k_{app\text{-}deocc}$ is exerted not only by Na^+ but also by K^+ and other monovalent cations. In this work, we have shown that Rb^+ competes with Na^+ for the site that promotes Rb^+-deocclusion, strongly suggesting that they bind to the same allosteric site. Under physiological conditions Na_e^+ and K_i^+ are present in concentrations high enough to maximally activate K^+-deocclusion and ATPase activity. If the allosteric site were intracellular, as suggested by the crystal structure of the intermediate occluded with Rb^+ (6, 7), then K_i^+ would be the main responsible for the activation effect. Crystallographic analysis showed an allosteric site for Rb^+ at about 30 Å from the two membranous transport sites towards the cytoplasmic side, in a binding cavity at the boundary between the P-domain and the transmembrane domain. Other authors also found kinetic evidence for an allosteric site for Na^+ although they claim it is on the extracellular face of the pump (48).

Since the allosteric modulation has a significant impact on the catalytic activity of the enzyme, studies of ligands for the allosteric site might have relevant pharmacological interest, whereas detailed kinetic studies in patients with some mental disorders may also lead to insights into the disease. In this sense, it is worth noting that Li^+, a cation that inhibits Rb^+-deocclusion (15), leads to an upregulatory response in the number of pump units in lymphocyte membranes of healthy patients, and this is not observed in patients with maniac-depressive psychosis (50–52). Whether the difference in these patients is due to alterations on the allosteric site requires further investigation.

EXPERIMENTAL PROCEDURES

Enzyme — We used a purified preparation of Na^+/K^+-ATPase inserted in open membrane fragments. This was obtained from pig kidney red-outer medulla by treatment of the microsomal fraction

with sodium dodecyl sulphate and extensive washing (53) based on the method of Jorgensen (54). The preparation was kindly provided by the Department of Biophysics, University of Århus, Denmark. Enzyme (abbreviated as Ez when present in the units) was quantified by measuring occluded Rb^+ under thermodynamic equilibrium in media containing 250 μM [^{86}Rb]RbCl, 0.25 mM EDTA and 25 mM imidazole-HCl (pH=7.4 at 25 °C). Under this condition, it is a good approximation to consider that every enzyme molecule occludes two Rb^+ ions. Using this stoichiometry, we obtained an average value of 2.51 ± 0.09 (nmol of Ez / mg protein) from four independent experiments.

Reagents and Reaction Conditions — [^{86}Rb]RbCl and [γ-^{32}P]ATP were from PerkinElmer Life Sciences. All other reagents were of analytical grade. Experiments were performed at 25 °C in media containing 2.5 mM ATP, 0.25 mM EDTA, 0 or 2 mM ADP, enough MgCl2 to give 0.5 mM free Mg^{2+}, 25 mM imidazole-HCl (pH=7.4 at 25 °C), and different concentrations of RbCl (instead of KCl), NaCl, and CholineCl so that the total concentration of the last three salts was always 170 mM.

ATPase activity (Act) — We determined ATPase activity from the time course of the release of [^{32}P]Pi from [γ-^{32}P]ATP, as in Monti et al. (33). Briefly, after the incubation time, we quenched the reaction, extracted the [^{32}P]Pi, and measured radiation due to Čerenkov effect in a scintillation counter. Despite we avoided hydrolysis of more than 10 % of the ATP initially present, we always checked that the release of Pi was linear with time in order to ensure initial rate conditions. These steady state determinations were made in media containing a protein concentration of 20 μg/ml and incubation times ranging from zero to 30 minutes. Reaction blanks were determined by measuring ATP hydrolysis in media containing 170 mM K^+, giving values not significantly different from those at 170 mM Na^+ and 1 mM ouabain (a specific inhibitor of Na^+/K^+-ATPase).

Specific concentration of occluded Rb^+ (Occ) — The methodology is described in Rossi et al. (55). Briefly, we employed a rapid-mixing apparatus (SFM4 from Bio-Logic, France) to start, incubate, and then squirt the reaction mixture at 2.5 ml/s into a quenching-and-washing chamber. There, the reaction is stopped by sudden dilution and cooling with an ice-cold solution of 30 mM KCl in 5 mM imidazole-HCl (pH=7.4 at 0 °C) flowing at 40 ml/s through a Millipore-type filter, where the enzyme is retained and washed. We measured the unspecific [^{86}Rb]Rb^+ binding to the filter by omitting the enzyme from the reaction medium. These values were similar to those obtained in the presence of enzyme inactivated either by heat (30 min at 65 °C) or by dilution 1/44 (final concentrations: 36 μg/ml of protein, 6 mM sucrose, 25 mM imidazole-HCl, 0.25 mM EDTA, pH=7.4 at 25 °C) and exposure to a freeze (-18 °C, overnight) and thaw cycle. Steady state determinations were made in media containing a protein concentration of 30-40 μg/ml, after an incubation time of 7 seconds.

Determination of the apparent velocity constant of Rb^+ deocclusion ($k_{app-deocc}$) — This was done by following the time course of Rb^+ deocclusion and fitting the equation

$$Occ(t) = Occ_{t=-q}\ e^{-k_{app\text{-}deocc}(t+q)}$$

where q is the time required to quench the reaction (8.0 ± 0.9 ms) and t is the incubation time. We obtained the Rb-occluded intermediates through the direct route of occlusion by incubation of the enzyme at 25 °C in a medium containing 0.10 mM [^{86}Rb] RbCl, 0.25 mM EDTA and 25 mM imidazole-HCl pH=7.4 for at least 20 min to achieve thermodynamic equilibrium. With the aid of the rapid mixing apparatus, we mixed 1 volume of the suspension (time zero) with 1 volume of media lacking [^{86}Rb] RbCl for different incubation times. Final concentrations were 2.5 mM ATP, 0.25 mM EDTA, 0.5 mM free Mg^{2+}, 25 mM imidazole-HCl pH=7.4, 0.05 mM (the minimal concentration attainable after the dilution) or 5 mM RbCl and different concentrations of NaCl, using CholineCl to keep constant the ionic strength. At the end of the incubation period, we quantified the Rb^+ that remained occluded. To determine the Rb^+ occluded at time zero, the suspension was diluted in a medium with 0.25 mM EDTA in 25 mM imidazole-HCl pH=7.4, a condition where Rb^+ deocclusion is very slow.

Empirical equations — For each [Rb^+] tested, we described steady-state measurements of ATPase activity and occluded Rb^+ by empirical equations of the form:

$$Act([Na^+]) = \frac{a_{Na0} + \sum_{j=1}^{n} a_{Naj} \frac{[Na^+]^j}{\prod_{g=1}^{j} K_{Nag}}}{denom} \quad (7)$$

and

$$Occ([Na^+]) = \frac{o_{Na0} + \sum_{j=1}^{m} o_{Naj} \frac{[Na^+]^j}{\prod_{g=1}^{j} K_{Nag}}}{denom} \quad (8)$$

where

$$denom = 1 + \sum_{j=1}^{d} \frac{[Na^+]^j}{\prod_{g=1}^{j} K_{Nag}}$$

and the parameters K_{Nag}'s are apparent stepwise dissociation constants expressed in concentration units, whereas the parameters a_{Naj}'s and o_{Naj}'s are coefficients with units of *Act* and *Occ*, respectively. All parameters where simultaneously fitted to the results by weighted nonlinear regression based on the Gauss-Newton algorithm using commercial programs (Excel, Sigma-Plot, and Mathematica for Windows). Weighting factors were calculated as the reciprocal of the variance of experimental data. We performed a systematic search of the equations that best describe the results for each $[Rb^+]$. First, we determined the degree of the polynomials in the numerator and the denominator. We restricted $n \leq d$ and $m \leq d$, to conform to steady-state equations for enzymes. Secondly, we evaluated the contribution of terms of intermediate degree by fixing some coefficient values to zero or establishing mathematical constraints between two or more coefficients. The goodness of fit of these equations was assessed by the corrected asymptotic information criterium (56) defined as:

$$AIC_c = nd \ln\left(\frac{SS_r}{nd}\right) + \frac{2(np+1)nd}{(nd-np-2)}$$

where nd is the number of data points, np is the number of parameters to be fitted, and SS_r is the sum of weighted square residual errors. We selected the equation that gave the minimum AIC_c value, since it is the one that describes the results using the minimum number of parameters.

We minimized the errors of the parameters by introducing constraints to their fitting values. For a given $[Rb^+]$ and [ADP], we obtained good fitting results by setting $a_{Na0} = a_{Na1} = a_{Na2}$ ($= a_{Na012}$), $o_{Na0} = o_{Na1} = o_{Na2}$ ($= o_{Na012}$), and $K_{Na1} = K_{Na2}$ ($= K_{Na12}$). These constraints are purely empirical. Additionally, for a given [ADP], we forced all equations to have the same ratio $a_{Na3}/(o_{Na3}/2)$. This constraint did not affect the capacity of equations to reproduce the results. It is based on equations from models as those in Figure 2 (see Equations S17 and S22, or S29 and S34 in Supplementary Material) and is independent of the nature of the transport mechanism.

Acknowledgments: In memory of Patricio J. Garrahan.

Conflict of interest: The authors declare that they have no conflicts of interest with the contents of this article.

Author contributions: JLEM contributed to the development of the analytical procedure used here to address non-Michaelis-Menten kinetics, designed and performed the experiments, analyzed the results, and wrote the paper. MRM contributed to the discussion of the results. RCR conceived the study, contributed to the development of the analytical procedure used here to address non-Michaelis-Menten kinetics, analyzed the results and wrote the paper. All authors reviewed the results and approved the final version of the manuscript.

REFERENCES

1. King, E. L. and Altman, C. (1956) A schematic method of deriving the rate laws for enzyme-catalyzed reactions, *J Phys Chem* **60**(10), 1375–1378.
2. Nomenclature Committee of the International Union of Biochemistry (NC-IUB) (1983) Symbolism and terminology in enzyme kinetics: recommendations 1981, *Arch Biochem. Biophys* **224**(2), 732–740.
3. Hill, C. M., Waightm, R. D., and Bardsley, W. G. (1977) Does any enzyme follow the Michaelis—Menten equation?, *Mol Cell Biochem.* **15**(3), 173–178.
4. Cleland, W. W. (1963) The kinetics of enzyme-catalyzed reactions with two or more substrates or products. III. Prediction of initial velocity and inhibition patterns by inspection, *Biochim Biophys Acta* **67**, 188–196.
5. Schulz, A. R. (1994) *Enzyme Kinetics: From Diastase to Multi-enzyme Systems*, Cambridge University Press, 1 edition
6. Shinoda, T., Ogawa, H., Cornelius, F., and Toyoshima, C. (2009) Crystal structure of the sodium-potassium pump at 2.4 A resolution, *Nature* **459**(7245), 446–450.
7. Schack, V. R., Morth, J. P., Toustrup-Jensen, M. S., Anthonisen, A. N., Nissen, P., Andersen, J. P., and Vilsen, B. (2008) Identification and function of a cytoplasmic K^+ site of the Na^+, K^+ -ATPase, *J Biol Chem* **283**(41), 27982–27990.
8. Kanai, R., Ogawa, H., Vilsen, B., Cornelius, F., and Toyoshima, C. (2013) Crystal structure of a Na^+-bound Na^+,K^+-ATPase preceding the E1P state, *Nature* **502**(7470), 201–206.
9. Nyblom, M., Poulsen, H., Gourdon, P., Reinhard, L., Andersson, M., Lindahl, E., Fedosova, N., and Nissen, P. (2013) Crystal structure of Na^+, K^+-ATPase in the Na^+-bound state, *Science* **342**(6154), 123.
10. Glynn, I. M. (1985) in *The Enzymes of Biological Membranes (AN Martonosi, ed.)* volume 3 pp. 35–114, Plenum Press, New York, 2nd edition
11. Glynn, I. M. (1993) Annual review prize lecture. 'All hands to the sodium pump', *J Physiol* **462**, 1–30.
12. Skou, J. C. and Esmann, M. (1992) The Na,K-ATPase, *J Bioenerg Biomembr* **24**(3), 249–261.
13. Sachs, J. R. (1980) The order of release of sodium and addition of potassium in the sodium-potassium pump reaction mechanism, *J Physiol* **302**, 219–240.
14. Sachs, J. R. (1986) The order of addition of sodium and release of potassium at the inside of the sodium pump of the human red cell, *J Physiol* **381**, 149–168.
15. Forbush, B. (1987) Rapid release of ^{42}K and ^{86}Rb from an occluded state of the Na^+,K^+-pump in the presence of ATP or ADP, *J Biol Chem* **262**(23), 11104–11115.
16. Forbush, B. (1984) Na^+ movement in a single turnover of the sodium pump, *Proc Natl Acad Sci U S A* **81**(17), 5310–5314.
17. Hoffman, P. G. and Tosteson, D. C. (1971) Active sodium and potassium transport in high potassium and low potassium sheep red cells, *J Gen Physiol* **58**(4), 438–466.
18. Garay, R. P. and Garrahan, P. J. (1973) The interaction of sodium and potassium with the sodium pump in red cells, *J Physiol* **231**(2), 297–325.
19. Chipperfield, A. R. and Whittam, R. (1976) The connexion between the ion-binding sites of the sodium pump, *J Physiol* **260**(2), 371–385.
20. Sachs, J. R. (1977) Kinetic evaluation of the Na^+-K^+ pump reaction mechanism, *J Physiol* **273**(2), 489–514.
21. Plesner, I. W. and Plesner, L. (1985) Kinetics of (Na^+ + K^+)-ATPase: analysis of the influence of Na^+ and K^+ by steady-state kinetics, *Biochim Biophys Acta* **818**(2), 235–250.
22. Plesner, L. and Plesner, I. W. (1985) Kinetics of Na^+-ATPase: influence of Na^+ and K^+ on substrate binding and hydrolysis, *Biochim Biophys Acta* **818**(2), 222–234.

23. Plesner, L. and Plesner, I. W. (1988) Exchange and hydrolysis kinetics of Na^+,K^+-ATPase, *Prog Clin Biol Res* **268A**, 335–340.
24. Plesner, L. and Plesner, I. W. (1988) Distinction between the intermediates in Na^+-ATPase and Na^+,K^+-ATPase reactions. I. Exchange and hydrolysis kinetics at millimolar nucleotide concentrations, *Biochim Biophys Acta* **937**(1), 51–62.
25. Plesner, L. and Plesner, I. W. (1988) Distinction between the intermediates in Na^+-ATPase and Na^+,K^+-ATPase reactions. II. Exchange and hydrolysis kinetics at micromolar nucleotide concentrations, *Biochim Biophys Acta* **937**(1), 63–72.
26. Garrahan, P. J. and Garay, R. P. (1976) in *Current Topics in Membranes and Transport* (Kleinzeller, F. B. a. A., ed) volume 8 pp. 29–97, Academic Press
27. Robinson, J. D. (1973) Variable affinity of the (Na^+ + K^+)-dependent adenosine triphosphatase for potassium. Studies using beryllium inactivation, *Arch Biochem. Biophys* **156**(1), 232–243.
28. Robinson, J. D. (1974) Cation interactions with different functional states of the Na^+,K^+-ATPase, *Ann N Y Acad Sci* **242**(0), 185–202.
29. Robinson, J. D. (1974) Affinity of the (Na^+ plus K^+)-dependent ATPase for Na^+ measured by Na^+-modified enzyme inactivation, *FEBS Lett* **38**(3), 325–328.
30. Segel, I. H. (1993) *Enzyme Kinetics: Behavior and Analysis of Rapid Equilibrium and Steady-State Enzyme Systems*, John Wiley & Sons, New York
31. Rossi, R. C. and Garrahan, P. J. (1989) Steady-state kinetic analysis of the Na^+/K^+-ATPase. The effects of adenosine 5'-[beta, gamma-methylene] triphosphate on substrate kinetics, *Biochim Biophys Acta* **981**(1), 85–94.
32. Glynn, I. M. (2002) A hundred years of sodium pumping, *Annu. Rev Physiol* **64**, 1–18.
33. Monti, J. L. E., Montes, M. R., and Rossi, R. C. (2013) Alternative cycling modes of the Na^+/K^+-ATPase in the presence of either Na^+ or Rb^+, *Biochim Biophys Acta* **1828**(5), 1374–1383.
34. Hara, Y. and Nakao, M. (1986) ATP-dependent proton uptake by proteoliposomes reconstituted with purified Na^+,K^+-ATPase., *J Biol Chem* **261**(27), 12655–12658.
35. Polvani, C. and Blostein, R. (1988) Protons as substitutes for sodium and potassium in the sodium pump reaction, *J Biol Chem* **263**(32), 16757–16763.
36. Blostein, R. (1985) Proton-activated rubidium transport catalyzed by the sodium pump, *J Biol Chem* **260**(2), 829–833.
37. Hara, Y., Yamada, J., and Nakao, M. (1986) Proton transport catalyzed by the sodium pump. Ouabain-sensitive ATPase activity and the phosphorylation of Na^+,K^+-ATPase in the absence of sodium ions, *J Biochem.* **99**(2), 531–539.
38. Lee, K. H. and Blostein, R. (1980) Red cell sodium fluxes catalysed by the sodium pump in the absence of K^+ and ADP, *Nature* **285**(5763), 338–339.
39. Blostein, R. (1983) Sodium pump-catalyzed sodium-sodium exchange associated with ATP hydrolysis, *J Biol Chem* **258**(13), 7948–7953.
40. Garrahan, P. J. and Glynn, I. M. (1967) The sensitivity of the sodium pump to external sodium, *J Physiol* **192**(1), 175–188.
41. Garrahan, P. J. and Glynn, I. M. (1967) The behaviour of the sodium pump in red cells in the absence of external potassium, *J Physiol* **192**(1), 159–174.
42. Karlish, S. J. and Glynn, I. M. (1974) An uncoupled efflux of sodium ions from human red cells, probably associated with Na^+-dependent ATPase activity, *Ann N Y Acad Sci* **242**(0), 461–470.
43. Glynn, I. M. and Karlish, S. J. (1976) ATP hydrolysis associated with an uncoupled sodium flux through the sodium pump: evidence for allosteric effects of intracellular ATP and extracellular sodium, *J Physiol* **256**(2), 465–496.
44. Kaufman, S. B., González-Lebrero, R. M., Rossi, R. C., and Garrahan, P. J. (2006) Binding of a single Rb^+ increases Na^+/K^+-ATPase, activating dephosphorylation without stoichiometric

occlusion, *J Biol Chem* **281**(23), 15721–15726.

45. Fedosova, N. U., Champeil, P., and Esmann, M. (2003) Rapid filtration analysis of nucleotide binding to Na^+,K^+-ATPase, *Biochemistry* **42**(12), 3536–3543.
46. Wong, J. T.-F. and Hanes, C. S. (1962) Kinetic formulations for enzymic reactions involving two substrates, *Can J Biochem. Physiol* **40**(6), 763–804.
47. Clarke, R. J., Humphrey, P. A., Lüpfert, C., Apell, H.-J., and Cornelius, F. (2003) Kinetic investigations of the mechanism of the rate-determining step of the Na^+,K^+-ATPase pump cycle, *Ann N Y Acad Sci* **986**, 159–162.
48. Garcia, A., Fry, N. A. S., Karimi, K., Liu, C.-c., Apell, H.-J., Rasmussen, H. H., and Clarke, R. J. (2013) Extracellular allosteric Na^+ binding to the Na^+,K^+-ATPase in cardiac myocytes, *Biophys J* **105**(12), 2695–2705.
49. Cornish-Bowden, A. (2014) Current IUBMB recommendations on enzyme nomenclature and kinetics, *Perspectives Sci.* **1**(1–6), 74–87.
50. Antia, I., Dorkins, C., Wood, A., and Aronson, J. (1992) Increase in Na^+/K^+-pump numbers in vivo in healthy volunteers taking oral lithium carbonate and further upregulation in response to lithium in vitro., *Br J Clin Pharmacol* **34**(6), 535–540.
51. Banerjee, U., Dasgupta, A., Rout, J. K., and Singh, O. P. (2012) Effects of lithium therapy on Na^+/K^+-ATPase activity and lipid peroxidation in bipolar disorder, *Prog Neuropsychopharmacol Biol Psychiatry* **37**(1), 56–61.
52. Marmol, F. (2008) Lithium: bipolar disorder and neurodegenerative diseases Possible cellular mechanisms of the therapeutic effects of lithium, *Prog Neuropsychopharmacol Biol Psychiatry* **32**(8), 1761–1771.
53. Klodos, I., Esmann, M., and Post, R. L. (2002) Large-scale preparation of sodium-potassium ATPase from kidney outer medulla, *Kidney Int* **62**(6), 2097–2100.
54. Jorgensen, P. L. (1975) Purification and characterization of (Na^+, K^+)-ATPase. V. Conformational changes in the enzyme Transitions between the Na^+-form and the K^+-form studied with tryptic digestion as a tool, *Biochim Biophys Acta* **401**(3), 399–415.
55. Rossi, R. C., Kaufman, S. B., González Lebrero, R. M., Nørby, J. G., and Garrahan, P. J. (1999) An attachment for nondestructive, fast quenching of samples in rapid-mixing experiments, *Anal Biochem.* **270**(2), 276–285.
56. Burnham, K. P. and Anderson, D. R. (2002) *Model selection and multimodel inference: a practical information-theoretic approach*, Springer, New York
57. Cha, S. (1968) A simple method for derivation of rate equations for enzyme-catalyzed reactions under the rapid equilibrium assumption or combined assumptions of equilibrium and steady state, *J Biol Chem* **243**(4), 820–825.

FOOTNOTES

This work was supported by Agencia Nacional de Promoción Científica y Tecnológica (PICT 2012 - 2014 1053), Consejo Nacional de Investigaciones Científicas y Técnicas (PIP 11220150100250CO), and Universidad de Buenos Aires (Ciencia y Técnica, grant 2014-2017 20020130100302BA), Argentina.

TABLES

Parameters equivalent to	Value of the parameters as $[Rb^+]$ tends to zero	
	Ping-pong	Ternary-complex
k_{cat}/K_M	> 0	$= 0$
K_M	$= 0$	> 0

Table 1: Ping-pong and ternary-complex patterns. Parameters equivalent to k_{cat}/K_M and K_M are, respectively, k_{catNai}/K_{MNai} and K_{MNai} in Equation 2, $a_{Nai3}/(K_{Nai1}K_{Nai2}K_{Nai3})$ and $K_{Nai1}K_{Nai2}K_{Nai3}$ in Equation 3, a_{Na1}/K_{Na1} and K_{Na1} in Equation 4, and $a_{Na3}/(K_{Na1}K_{Na2}K_{Na3})$ and $K_{Na1}K_{Na2}K_{Na3}$ in Equation 5.

Parameter	Value ± SE	Units
k_{deocc}	10.4 ± 0.9	s^{-1}
$k_{deoccna}$	23.4 ± 0.8	s^{-1}
K_{Na}	8 ± 4	mM

Table 2: Fitted values of parameters of the model in Figure 5B

[ADP]	[Rb^+]	a_{Na012}	a_{Na3}	a_{Na4}	a_{Na5}	K_{Na12}	K_{Na3}	K_{Na4}	K_{Na5}	o_{Na012}	o_{Na3}	o_{Na4}	$a_{Na3}/(K_{Na1}K_{Na2}K_{Na3})$	$K_{Na1}K_{Na2}K_{Na3}$	$a_{Na3}/(o_{Na3}^2)$	$a_{Na4}/(o_{Na4}^2)$
(mM)	(mM)	(mol Pi/(mol Ez·s))				(mM)				(mol Rb^+/mol Ez)			((mol Pi/(mol Ez·s))/mM^3)	(mM^{-3})	(s^{-1})	(s^{-1})
0	0.035	0.19 ± 0.03	3.02 ± 0.55	0.32 ± 0.07	$6.6 \cdot 10^3 \pm 8.4 \cdot 10^4$	0.2 ± 0.1	0.9 ± 0.3	1.2 ± 0.3	$1.1 \cdot 10^6 \pm 1.4 \cdot 10^7$	0.044 ± 0.001	0.60 ± 0.11	0.004 ± 0.001	132 ± 64	0.02 ± 0.01	10.1 ± 0.2	146 ± 41
0	0.120	0.28 ± 0.03	5.16 ± 0.45	1.76 ± 0.13	$1.2 \cdot 10^4 \pm 7.8 \cdot 10^4$	0.3 ± 0.1	1.1 ± 0.2	4.6 ± 0.7	$2.5 \cdot 10^6 \pm 1.7 \cdot 10^7$	0.066 ± 0.001	1.03 ± 0.09	0.027 ± 0.004	67 ± 20	0.08 ± 0.02	"	130 ± 20
0	0.245	0.32 ± 0.03	7.17 ± 0.37	3.91 ± 0.26	$5.7 \cdot 10^4 \pm 8.3 \cdot 10^4$	0.6 ± 0.1	0.8 ± 0.1	13.7 ± 1.9	$1.4 \cdot 10^7 \pm 1.6 \cdot 10^7$	0.091 ± 0.002	1.42 ± 0.07	0.158 ± 0.014	28 ± 5	0.25 ± 0.04	"	50 ± 6
0	0.500	0.25 ± 0.03	7.11 ± 0.42	9.32 ± 0.59	0.5 ± 8.5	1.0 ± 0.4	0.6 ± 0.1	14.2 ± 5.2	$8.8 \cdot 10^2 \pm 7.8 \cdot 10^2$	0.165 ± 0.004	1.41 ± 0.08	0.648 ± 0.107	11 ± 3	0.64 ± 0.13	"	29 ± 6
0	1	0.30 ± 0.03	6.20 ± 0.20	12.67 ± 0.17		1.3 ± 0.5	0.4 ± 0.1	15.1 ± 1.5		0.328 ± 0.005	1.23 ± 0.03	0.803 ± 0.017	10 ± 2	0.63 ± 0.11	"	31.5 ± 0.9
0	3	0.16 ± 0.02	8.04 ± 0.28	15.85 ± 0.21		1.3 ± 0.3	0.6 ± 0.1	20.1 ± 2.3		0.883 ± 0.010	1.60 ± 0.04	1.420 ± 0.027	7 ± 1	1.08 ± 0.15	"	22.3 ± 0.6
0	5	0.11 ± 0.03	8.29 ± 0.33	15.57 ± 0.20		1.5 ± 0.6	0.8 ± 0.1	17.2 ± 2.5		1.213 ± 0.010	1.65 ± 0.06	1.409 ± 0.027	5 ± 1	1.79 ± 0.44	"	22.1 ± 0.6
2	0.010	0.07 ± 0.02	0.80 ± 0.42	0.03 ± 0.03	$1.4 \cdot 10^3 \pm 4.8 \cdot 10^4$	0.3 ± 0.4	1.0 ± 1.0	0.8 ± 0.5	$3.1 \cdot 10^6 \pm 1.0 \cdot 10^7$	0.033 ± 0.002	0.16 ± 0.14		11 ± 12	0.07 ± 0.06	5.8 ± 0.1	
2	0.020	0.08 ± 0.03	1.87 ± 1.23			0.4 ± 0.4	1.4 ± 1.5	1.2 ± 1.1		0.040 ± 0.002	0.37 ± 0.42	0.026 ± 0.017	10 ± 7	0.19 ± 0.10	"	
2	0.035	0.04 ± 0.02	2.78 ± 0.78	0.02 ± 0.05	$5.4 \cdot 10^3 \pm 8.9 \cdot 10^4$	0.3 ± 0.2	2.1 ± 0.9	1.7 ± 0.6	$9.0 \cdot 10^6 \pm 1.5 \cdot 10^7$	0.046 ± 0.003	0.55 ± 0.27	0.007 ± 0.002	13 ± 8	0.22 ± 0.10	"	7 ± 14
2	0.060	0.11 ± 0.04	3.22 ± 0.87	0.09 ± 0.21		0.5 ± 0.4	1.5 ± 0.7	4.2 ± 2.3		0.053 ± 0.004	0.64 ± 0.30	0.012 ± 0.055	8 ± 4	0.42 ± 0.15	"	14 ± 39
2	0.120	0.12 ± 0.02	3.17 ± 0.30	1.00 ± 0.18		0.8 ± 0.3	1.2 ± 0.3	9.6 ± 1.7		0.068 ± 0.003	0.63 ± 0.10	0.036 ± 0.009	5 ± 1	0.69 ± 0.16	"	55 ± 18
2	0.245	0.13 ± 0.02	2.67 ± 0.12	2.97 ± 0.15		1.3 ± 0.5	0.7 ± 0.1	30.8 ± 5.6		0.095 ± 0.004	0.53 ± 0.04	0.080 ± 0.028	2.4 ± 0.5	1.12 ± 0.22	"	74 ± 27
2	1	0.12 ± 0.03	1.91 ± 0.12	6.25 ± 0.19		3.0 ± 3.3	0.3 ± 0.2	7.6 ± 1.3		0.322 ± 0.007	0.38 ± 0.04	0.549 ± 0.013	0.8 ± 0.3	2.48 ± 0.99	"	22.8 ± 0.9
2	3	0.06 ± 0.02	2.28 ± 0.10	7.30 ± 0.21		4.5 ± 5.1	0.3 ± 0.2	10.1 ± 1.9		0.888 ± 0.014	0.45 ± 0.03	0.728 ± 0.017	0.4 ± 0.1	5.51 ± 2.00	"	20.1 ± 0.8
2	5	0.03 ± 0.03	2.66 ± 0.09	8.04 ± 0.34		5.1 ± 5.7	0.4 ± 0.3	20.1 ± 4.6		1.189 ± 0.017	0.53 ± 0.02	0.785 ± 0.021	0.3 ± 0.1	9.22 ± 4.06	"	20.5 ± 1.2

Table 3: Fitted values (± SE) of parameters in empirical equations (Equations 7 and 8) to the results obtained at different [Rb^+] and [ADP].

FIGURES

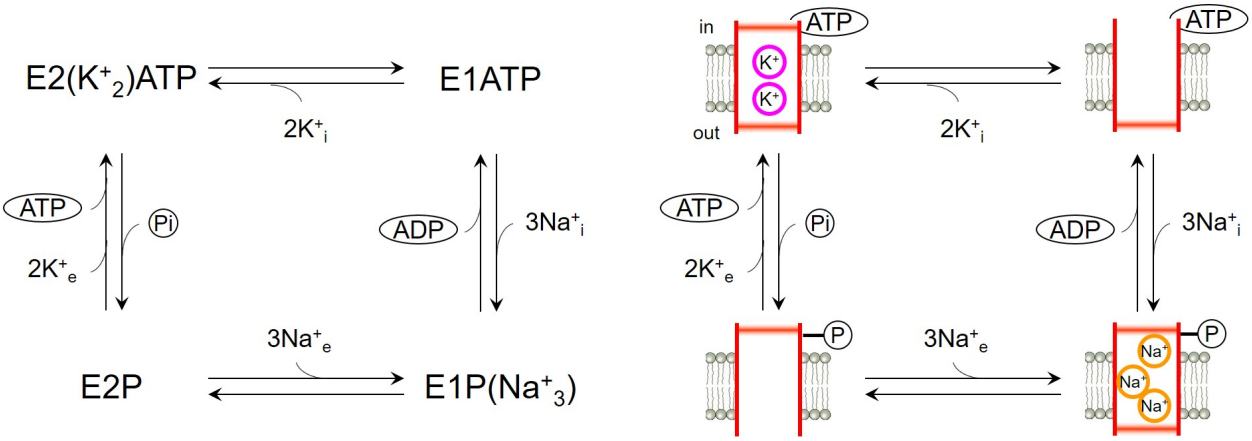

Figure 1: A simplified version of the Albers-Post model for the physiological functioning of Na^+/K^+-ATPase. The reaction scheme (left) has been cartooned (right) for better comprehension. Subscripts *i* and *e* are for intracellular and extracellular respectively. For the diagram on the left, occluded cations are written within parentheses. For the diagram on the right, each intermediate is represented with its cytoplasmic side (*in*) facing up. Under physiological conditions, the reaction cycle proceeds clockwise.

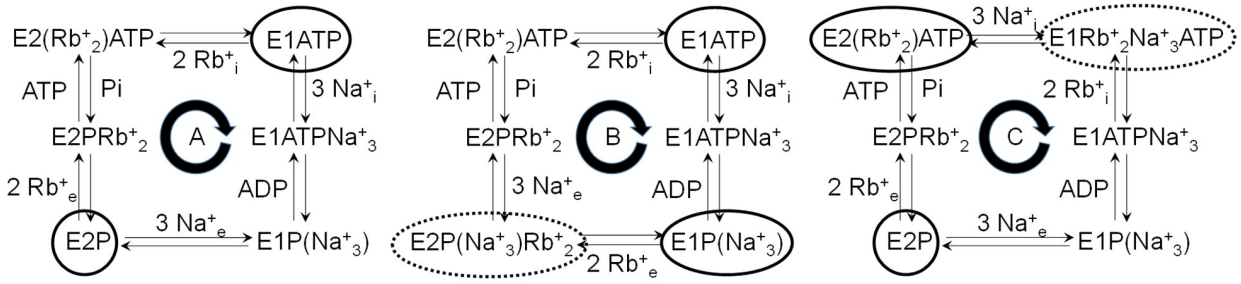

Figure 2: Ping-pong (A) and ternary-complex (B and C) models for the transport mechanism of Na^+/K^+-ATPase. The reaction proceeds clockwise. Ellipses in continuous lines enclose the reaction intermediates that bind cations as substrates (Na_i^+ and Rb_e^+). Ellipses in dotted lines enclose ternary complexes.

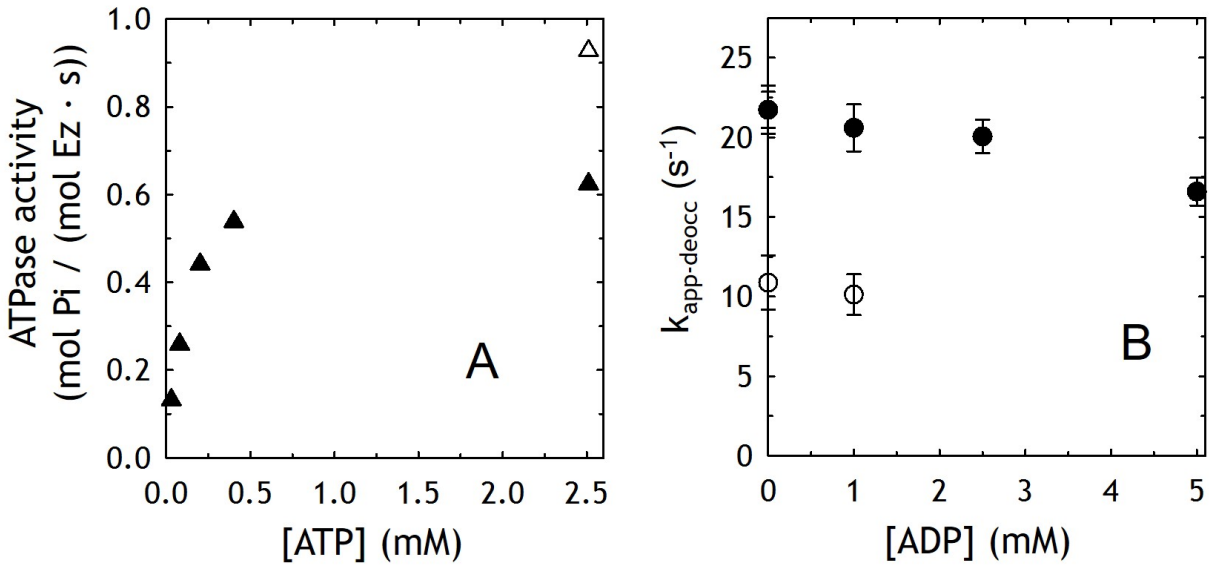

Figure 3: Effects of ADP on the substrate curve of the Na^+-ATPase activity and on the rate of Rb^+-deocclusion. Reaction media contained 0.25 mM EDTA, 0.5 mM Mg^{2+} free, 25 mM imidazole-HCl pH= 7.4 and CholineCl to keep constant ionic strength. Panel A: Na^+-ATPase activity was measured in the presence of 170 mM NaCl and 2 mM ADP (filled triangles). One determination was performed at 2.5 mM ATP in the absence of ADP (empty triangle). Panel B: $k_{app\text{-}deocc}$ measured at 2.5 mM ATP in the abscence (empty circles) and in the presence of 170 mM Na^+ (filled circles). Vertical bars are ± Standard Error (SE).

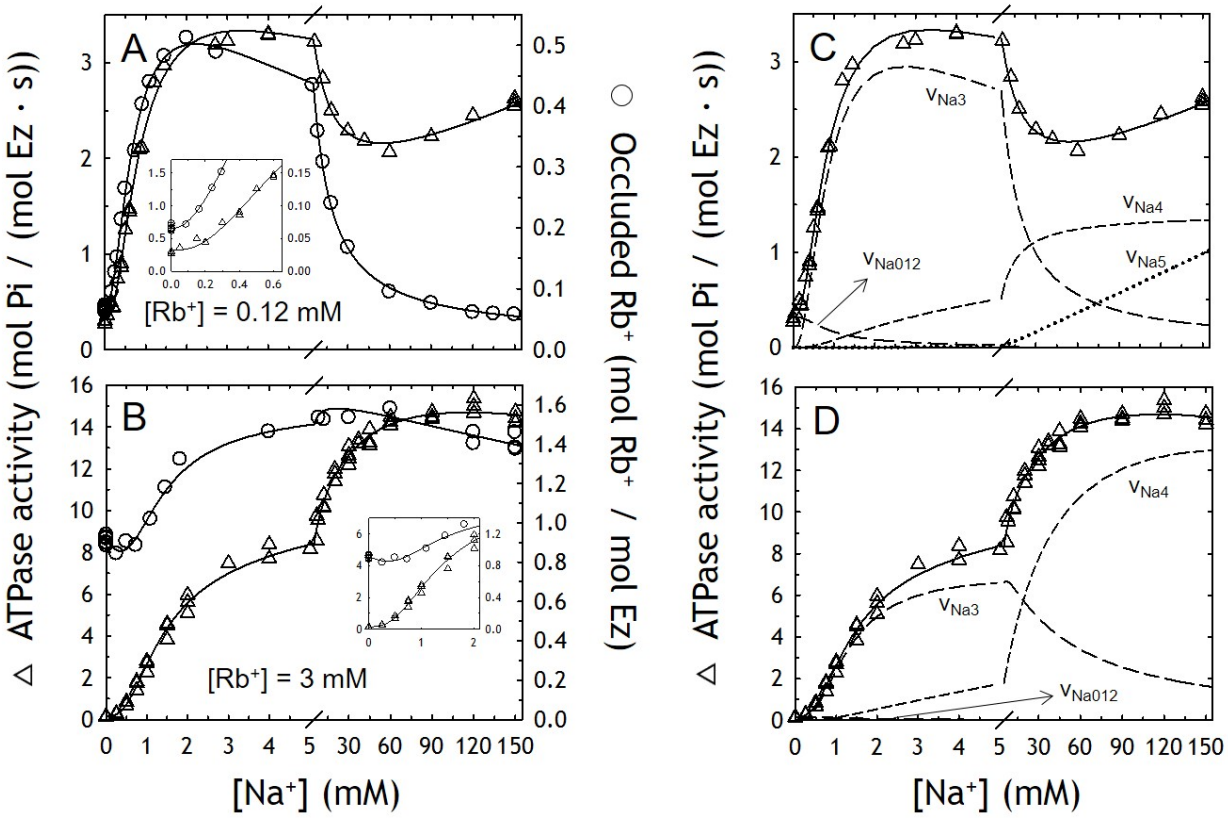

Figure 4: Typical curves of *Act* and *Occ* as a function of [Na^+] at *low* (panel A) and *high* (panel B) [Rb^+] and the analysis of *Act* (panels C and D) in terms of v_{Na_j} (see Equation 6). We show results for ATPase activity (△) and steady-state levels of occluded Rb^+ (○) at 0.12 (panels A and C) and 3 (panels B and D) mM RbCl. Solid lines are the plot of the empirical equations that gave the best fit to the results (see main text). Dotted/dashed lines are the contribution of each v_{Na_j} term to *Act*. Note that contribution of v_{Na012} to *Act* is negligible for most Na^+ concentrations.

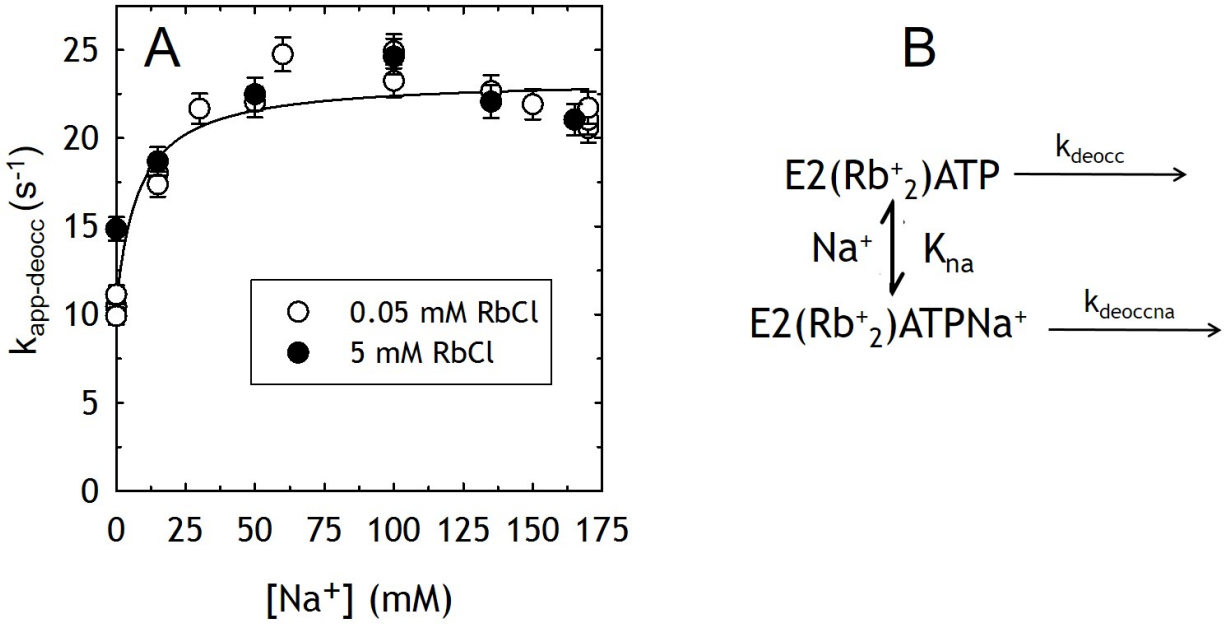

Figure 5: Effect of [Na^+] on the apparent velocity constant of Rb^+ deocclusion. Panel A shows $k_{app\text{-}deocc}$ values measured at 0.05 (○) and 5 (●) mM RbCl. Vertical bars are ± SE. The solid line is the best fit to the results of the equation $k_{app\text{-}deocc} = \left(k_{deocc} + \frac{k_{deoccna}[Na^+]}{K_{Na}}\right) \Big/ \left(1 + \frac{[Na^+]}{K_{na}}\right)$, which is given by the model shown in panel B. In panel B, k_{deocc} and $k_{deoccna}$ are the velocity constants of Rb^+ deocclusion when the allosteric site is free or occupied by Na^+, respectively; whereas K_{Na} is the dissociation constant of the allosteric site for Na^+. Best fitting values of parameters of model in panel B are given in Table 2.

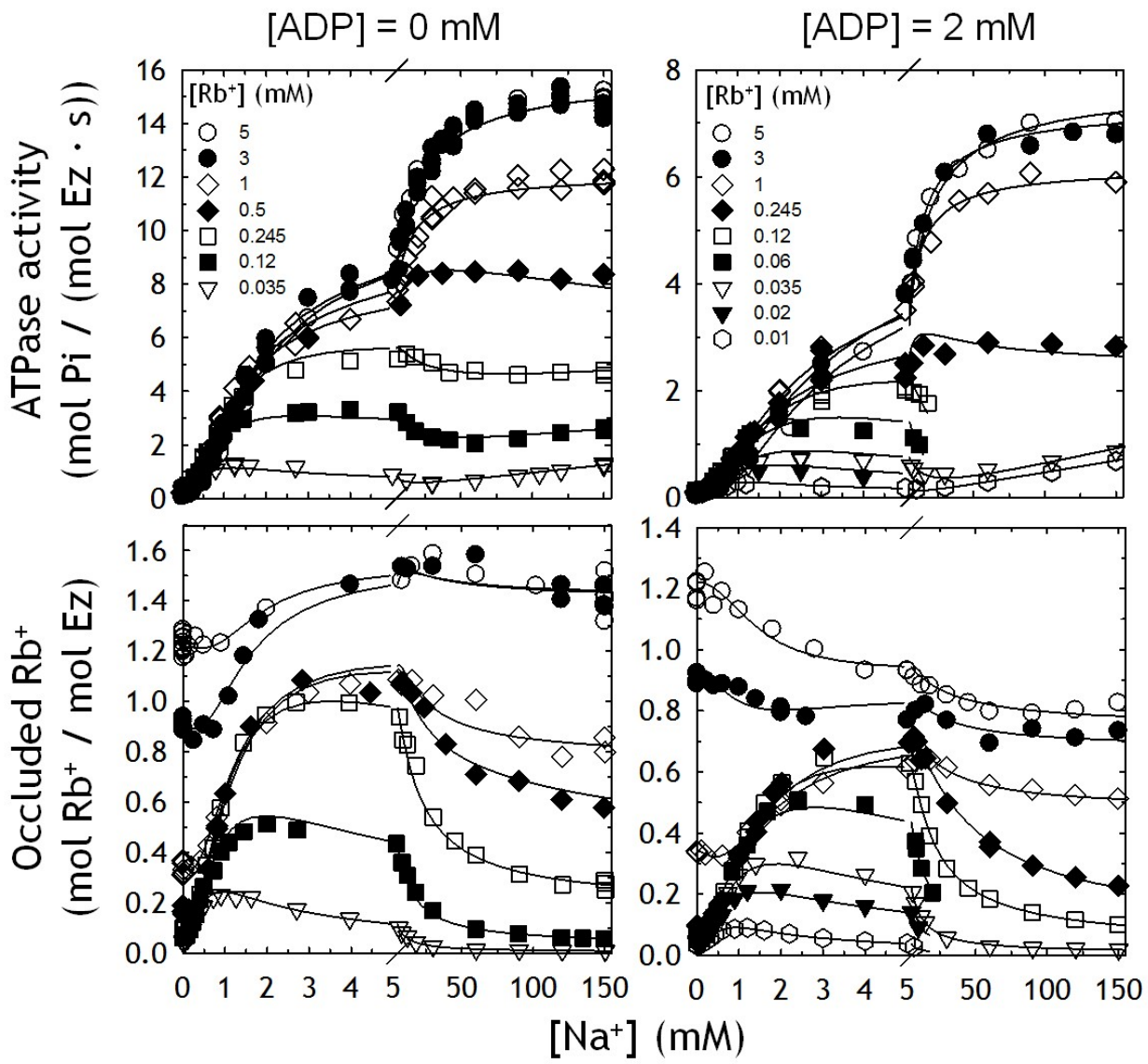

Figure 6: Empirical fit to the results. Solid lines are the plot of the empirical Equations 7 and 8 with the constraints specified under *Empirical equations*. Best fitting values of the parameters are shown in Table 3.

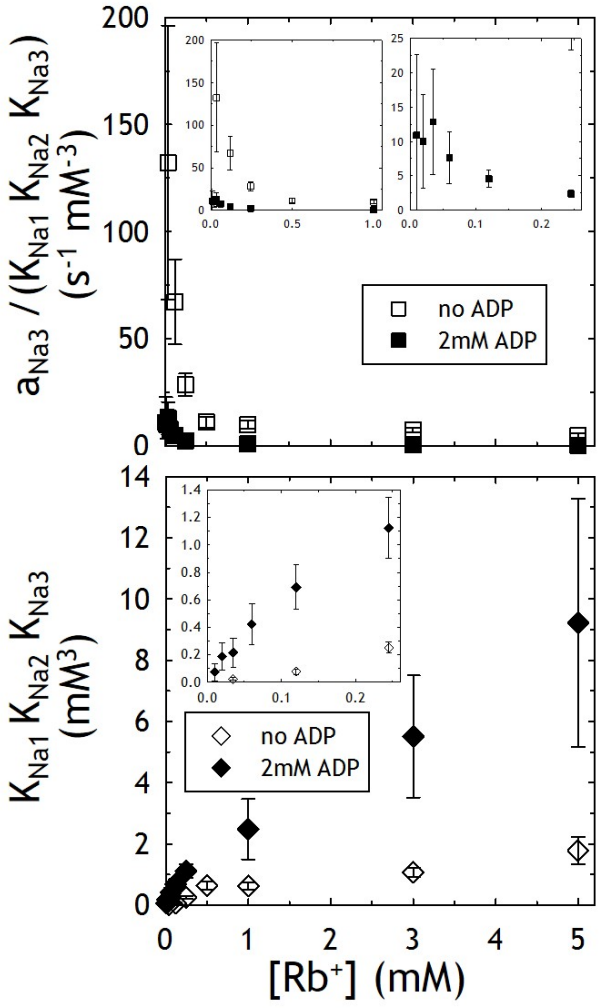

Figure 7: Dependence of the parameters $a_{Na3}/(K_{Na1}K_{Na2}K_{Na3})$ (upper panel) and $K_{Na1}K_{Na2}K_{Na3}$ (lower panel) with the fixed concentration of Rb^+ in the absence (empty symbols) and in the presence of 2 mM ADP (filled symbols). Vertical bars are ± SE. Insets show more clearly the results obtained at low Rb^+ concentrations.

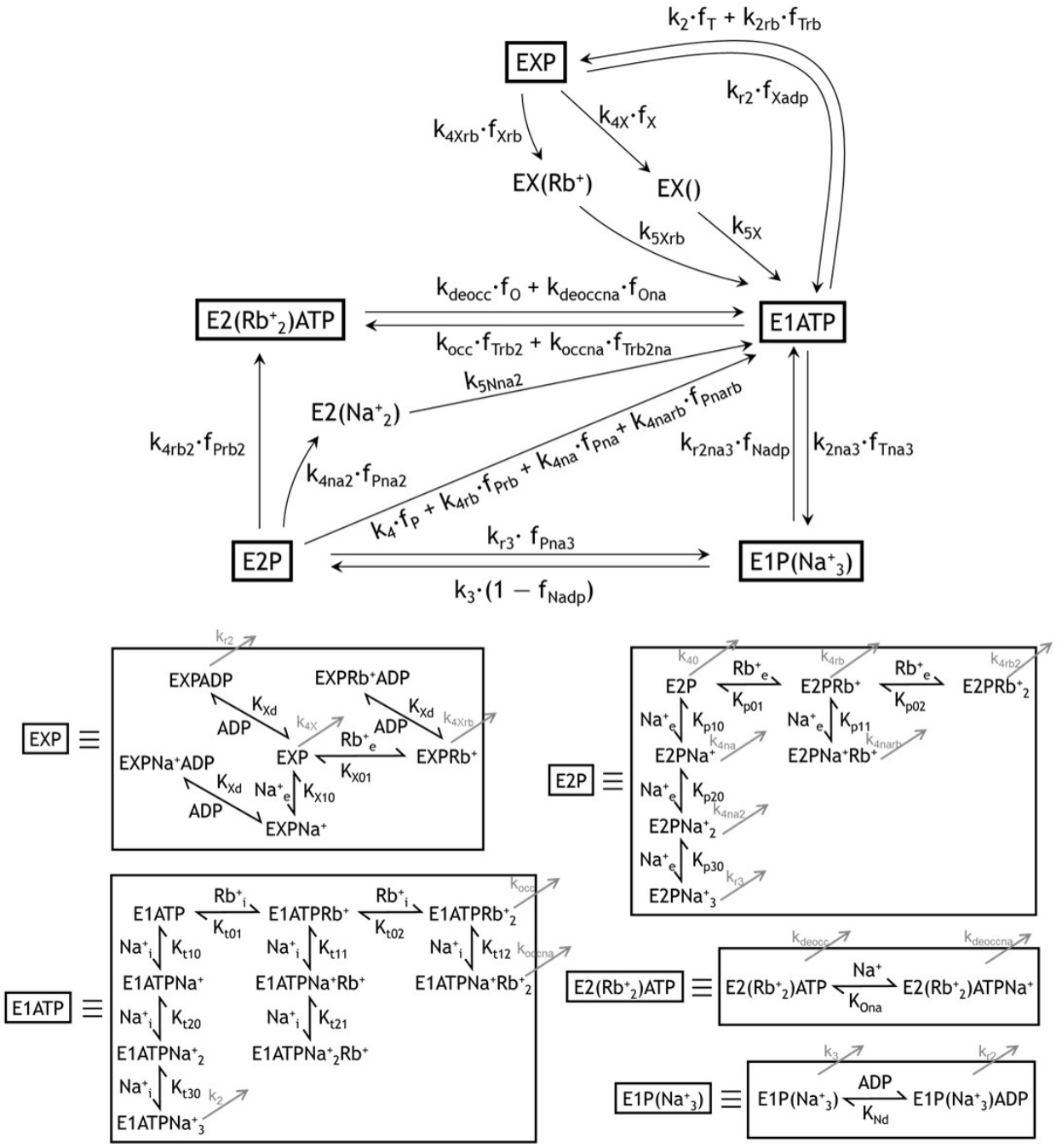

Figure 8: A ping-pong model of the kinetic mechanism of Na^+/K^+-ATPase. Reaction intermediates within a rapid equilibrium segment are grouped (see (57)) and included into a box. Intermediates within each box are explicitly shown below the model. k's are rate constants and K's are equilibrium dissociation constants. The f's represent the fractional concentration of an intermediate within the box. The model includes the alternative cycling modes of functioning. There are two phosphorylation pathways: the physiological one to give E1P(Na^+_3) and another that takes place in the absence of Na^+ to give EXP (see (33)). E2P dephosphorylation is strongly stimulated by the binding of 2 Rb^+ (f_{Prb2}). Dephosphorylation can also occur at a slow rate through any of the following reactions: (i) spontaneously (f_P) or after the binding of (ii) 2 Na^+ (f_{Pna2}), (iii) 1 Rb^+ (f_{Prb}), (iv) 1 Na^+ (f_{Pna}), or (v) 1 Na^+ and 1 Rb^+ (f_{Pnarb}). The deocclusion of Rb^+ from E2(Rb^+_2)ATP is the main rate limiting step of the physiological cycle, and leads to E1ATP either spontaneously (f_O) or after the binding of Na^+ to an allosteric site (f_{Ona}). Dephosphorylation is considered irreversible because of the absence of Pi. It is worth mentioning that a good fit was obtained even by assigning values of zero to k_{4na} and k_{4rb} (see Table S1 in Supplementary Material).

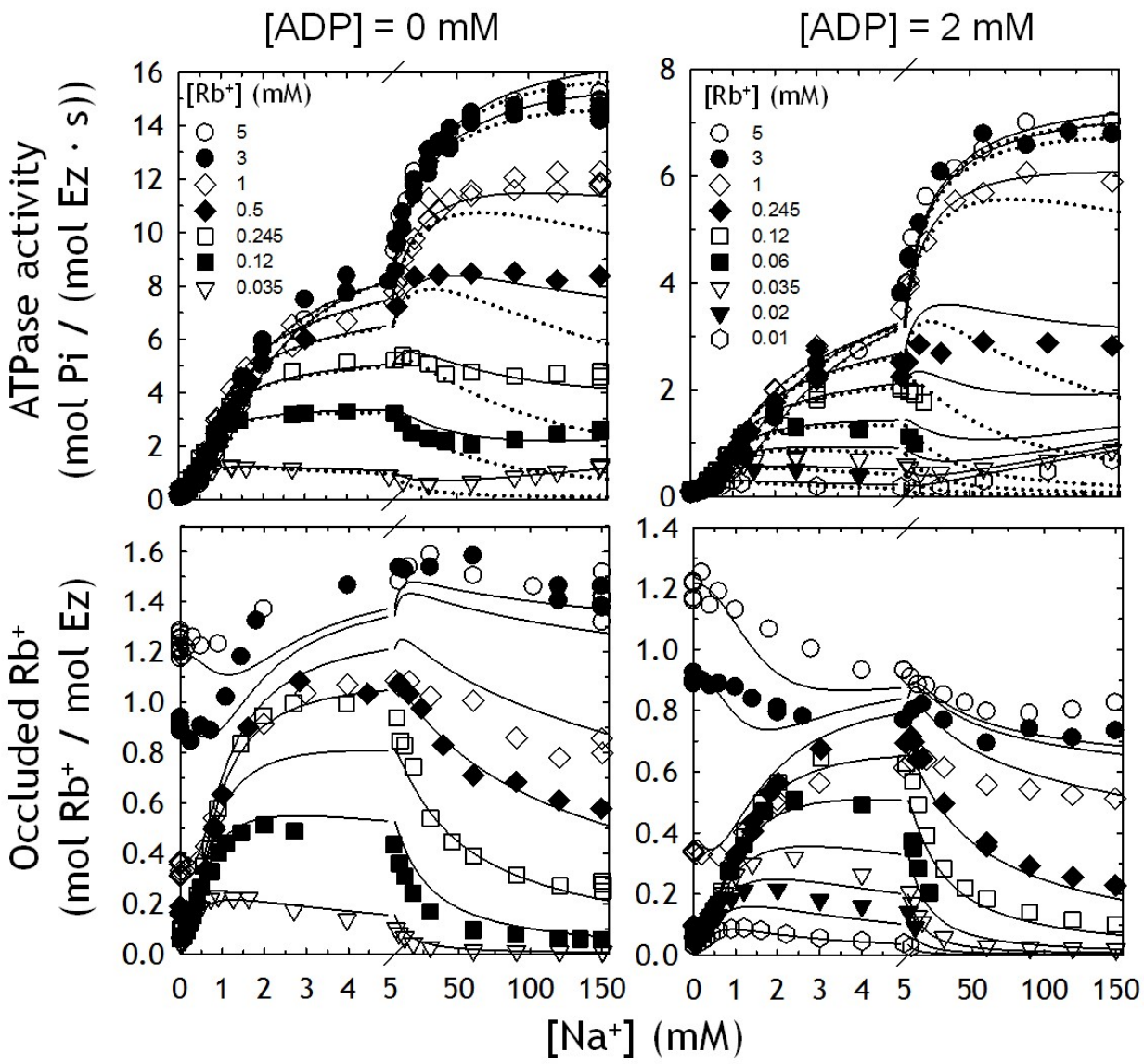

Figure 9: Fit of the model in Figure 8 to the results. The continuous lines are the plot of the equations corresponding to the model in Figure 8 for the parameters values shown in Table S1 in Supplementary Material. The dotted lines are the plot of the contribution to *Act* of the physiological flux.

Steady-state analysis of enzymes with non-Michaelis-Menten kinetics. The transport mechanism of Na^+/K^+-ATPase.

José L. E. Monti, Mónica R. Montes and Rolando C. Rossi

J. Biol. Chem. published online November 30, 2017

Access the most updated version of this article at doi: 10.1074/jbc.M117.799536